Sequential calibration of material model using mixed-effects

Clément Laboulfie, Mathieu Balesdent, Loïc Brevault, François-Xavier Irisarri, Jean-François Maire, Sebastien da Veiga, Rodolphe Le Riche

Sequential calibration of material model using mixed-effects

C. LABOULFIE[a], M. BALESDENT[b], L. BREVAULT[b], F.-X. IRISARRI[a], J.-F. MAIRE[a], S. DA VEIGA[c], R. LE RICHE[d]

a. DMAS, ONERA, Université Paris Saclay F-92322, Châtillon FRANCE
clement.laboulfie,francois-xavier.irisarri,jean-francois-maire@onera.fr
b. DTIS, ONERA, Université Paris Saclay F-91123, Palaiseau FRANCE
mathieu.balesdent,loic.brevault@onera.fr
c. Safran TECH Rue des jeunes Bois, 78117 Châteaufort FRANCE
sebastien.da-veiga@safrangroup.com
d. LIMOS (CNRS, Mines Saint-Étienne & UCA), FRANCE
leriche@emse.fr

Abstract

This paper presents a new sequential method to calibrate a material model in the presence of significant material variability. Material variability is handled in the mixed-effects framework. In this approach, material variability is described by a probability distribution calibrated by maximizing a likelihood. Yet, when the number of model parameters or the computational time of a single run of the models increases (for multiaxial models for instance), the maximization of the likelihood of mixed-effects is more difficult to perform. Furthermore, the parameters do not have the same influence on the material model depending on the nature of the test. The proposed procedure enables to calibrate the model on multiple experiments. It relies on the definition of a sequence of calibration subproblems. Associated to the relevant experimental data, each subproblem allows to calibrate the joint distribution of a subset of the model parameters. The maximization of the attached likelihood is eased as the number of unknown parameters is reduced compared to full problem. The subproblems are solved sequentially. To ensure consistency of the global process, the research space for the distribution parameters already estimated with a previous calibration is restricted to a trust region. The proposed calibration process is applied to an orthotropic elastic model with laminates made from T700GC/M21 base ply material. The ability of the procedure to sequentially estimate the model parameters distribution is investigated. Its capability to ensure consistency throughout the calibration process is discussed. Results show that the proposed procedure is a promising methodology to handle the calibration of complex material models in the mixed-effects framework.

Keywords : Mixed-effects models, Model Calibration, Composites Material, Sequential Calibration

1 Introduction

Following the increase of numerical facilities, virtual testing is now widely used in order to partially substitute numerical simulations to experimental campaigns because of time and costs considerations.

These numerical simulations require the use of material models which describe different phenomena such as elasticity, viscosity, damage, *etc.* These models involve several parameters that need to be calibrated. Calibrating model parameters consists in finding the parameters value that allow to best fit the experimental responses of interest. Yet, this task is challenging because the model may not be able to fully reproduce the observations, the experimental data can be noisy and the material properties subject to inherent variability. Consequently, a faithful calibration of the model parameters requires to take into account the different sources of uncertainty in the identification process.

The properties of composite materials are known to be subjected to a significant variability because of the complexity of the production process. To characterize this variability, international standards impose to perform test repetitions [7] to determine the model parameters distribution. The model parameters are calibrated independently on several specimens by minimizing a fitting criterion [27] before inferring the model parameters distribution by maximizing a likelihood [29]. Yet, this procedure is not fully satisfying because the fitting criterion (*e.g.*, least-square, log-likelihood [1, 29]) does not consider material variability in its definition. To overcome this difficulty, Laboulfie *et al.* [18] proposed the use of mixed-effects models [8, 20], a population-based approach, to characterize material variability. The mixed-effects notion comes from the fact that there are "fixed" effects that are shared by the entire population of individuals (*i.e.* specimen) and "random" effects that are specific to each individual of the population. For instance, the Young's modulus measured on a tensile test specimen can be considered as the combination of a reference value (the average value given by the manufacturer for a material batch) and of a deviation due to the variability of the production process. The mixed-effects approach assumes that the model parameters describing the different specimens, known as the individual parameters, are distributed according to a joint probability distribution (*e.g.*, a multivariate Gaussian distribution). This distribution represents the impact of material variability on the model parameters. The parameters of this distribution are determined by a likelihood maximization. This kind of approaches has already been applied successfully to calibrate simple material models [18].

More complex models involve the combination of several phenomena (elasticity, failure, damage viscosity, *etc.*) to which are attached specific parameters. They also describe in-plane and out-of-plane behaviors. Thus, the model to calibrate usually involves many parameters, increasing the size of the research space and making the optimization of the likelihood more difficult. Furthermore, the computation of the likelihood of the mixed-effects is challenging as this likelihood expresses as a product of multivariate integrals. Given the computational time of a single run of those models (especially for multi-scale non-linear models), the estimation of the likelihood requires to set up appropriate strategies (*e.g.* meta-modeling). Therefore, in order to decrease the complexity of the calibration in the presence of uncertainty, it could be interesting to take advantage of the decomposition of the model to transform the large calibration problem into a sequence of appropriate smaller calibration sub-problems, corresponding to the different test configurations (*e.g.* different load profiles and stacking sequences). In addition to decrease the number of parameters to be identified, it alleviates the computational costs as it allows to not to take into account all the phenomena at the same time.

To calibrate the material parameters, often, we dispose of experimental tests of different natures either in terms of loads (*e.g.*, traction, compression or shear tests) or in terms of stacking sequences (*e.g.* uni-directional laminate 0° or quasi-isotropic laminates). Nevertheless, the sensitivity of the model

output with respect to the model parameters depends on the nature of the test [4] and all model parameters characterizing a given phenomenon (elasticity for instance) cannot always be estimated with the same type of test. Consequently, if it is decided to calibrate sub-problems, the choice of the relevant parameters must be performed carefully to avoid ill-posed problems.

To solve such problems, we propose in this paper a sequential procedure to calibrate mechanical models compliant with the mixed-effects framework. This procedure aims to calibrate the same orthotropic elastic model on multiple experiments with different stacking sequences. Prior to calibration, for each available specimen, the parameters to which the model output is sensitive are determined from expert knowledge. This allows to define a sequence of calibration problems with a separation of the calibrated parameters. Note that the separation is not strict as some parameters may be sensitive on several tests. For a given calibration sub-problem (transformed into an optimization problem) attached to the appropriate experimental data, only the joint distribution and the realizations corresponding to the relevant parameters is estimated. To ensure consistency between the different steps of the sequential calibration process, for a given step, the research space of the distribution parameters already estimated with previous calibrations is limited to a trust region. The distribution parameters of the model coefficients that are not sensitive are fixed during the resolution of this calibration sub-problem.

This paper is organized as follows. Section 2 introduces mixed-effects for model calibration, with a focus on the treatment of multivariate data. In Section 3, the proposed sequential calibration process is presented in details. In order to illustrate the performance of the calibration technique, the methodology is applied to the calibration of a orthotropic elastic model with laminates made from T700GC/M21 base ply material in Section 4 before concluding in Section 5.

2 Mixed-effects for calibration

First, let us recall that the material model calibration aims, for a given a material model $\mathcal{F}(\cdot, \boldsymbol{\theta})$, to find a set of model parameters labeled $\boldsymbol{\theta} \in \mathbb{R}^d$ (d standing for the number of parameters to be calibrated) which allows to mimic the experimental data. The calibration problem in the presence of uncertainty can be formalized as follows [11, 15]. Let us note the random vector of the output data Y and $\mathbf{y} = (y_j)_{j \in [\![1,N]\!]}$ its outcome, with N the number of observations, considering one specimen. Classically, the following decomposition applies : [11, 15]

$$\mathbf{y} \sim \mathcal{F}(\cdot, \boldsymbol{\theta}) + \boldsymbol{\xi} \, , \tag{1}$$

where $\boldsymbol{\xi}$ stands for the random vector of the errors which represents the experimental noise and the model bias. The outcomes of $\boldsymbol{\xi}$ can be different from one measure to the other and are labeled $(\xi_j)_{j \in [\![1,N]\!]}$. Eq.(1) can be further detailed :

$$y_j \coloneqq \mathcal{F}(t_j, \boldsymbol{\theta}) + \xi_j \, , \tag{2}$$

with t_j the j^{th} input measure, which is deterministic.

Mixed-effects models are a population-based approach that explicitly models the variability between individuals within a population. Figure 1 illustrates this fundamental difference with respect to the classical approaches summarized previously.

In the classical approaches (Figure 1.a), individual variability is neglected and combined with other types of uncertainties, which allows to describe all the specimens by the same vector of model parameters. In

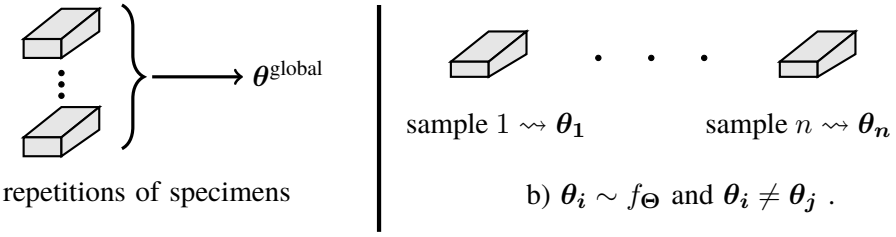

a) repetitions of specimens

b) $\boldsymbol{\theta_i} \sim f_{\boldsymbol{\Theta}}$ and $\boldsymbol{\theta_i} \neq \boldsymbol{\theta_j}$.

Figure 1: Difference between the population and the classical approaches. On the left, a), usual methods with a single parameter vector for all specimens. On the right, b), population-based approach in the mixed-models effects framework.

the mixed-effects approach (Figure 1.b), each sample is assigned a specific parameter vector value called the individual parameters. It is assumed that there exists an underlying probability distribution $f_{\boldsymbol{\Theta}}$ whose outcomes are the individual parameters $(\boldsymbol{\theta_i})_{i\in[\![1,n]\!]}$ with n the number of individuals [8, 20]. Both the underlying probability distribution of the model parameters and the value of the individual parameters are determined. In addition, it remains possible to take into account other sources of uncertainty, such as measurement noise. Thus, mixed-effects models are particularly well suited to situations in which individual variability cannot be neglected with respect to other sources of uncertainty.

2.1 Formalization

The mixed-effects framework [8, 20] assumes that there exists a probability distribution $f_{\boldsymbol{\Theta}}$ whose outcomes are the individual parameters:

$$\forall i \in [\![1, n]\!],\ \boldsymbol{\theta_i} \underset{\text{i.i.d.}}{\sim} f_{\boldsymbol{\Theta}} \ . \tag{3}$$

Both $f_{\boldsymbol{\Theta}}$ and the $\boldsymbol{\theta_i}$ are unknown and the aim is to determine them. In addition, if $f_{\boldsymbol{\Theta}}$ is parametric (a Gaussian distribution for instance), let $\boldsymbol{\Pi}$ be its parameters and $f_{\boldsymbol{\Theta}} = f_{\boldsymbol{\Theta},\boldsymbol{\Pi}}$. Identifying $f_{\boldsymbol{\Theta},\boldsymbol{\Pi}}$ is tantamount to determining $\boldsymbol{\Pi}$. Given $\boldsymbol{\Pi}$ and $\boldsymbol{\theta_i} \sim f_{\boldsymbol{\Theta},\boldsymbol{\Pi}}\ \forall i \in [\![1, n]\!]$, the model output $\mathbf{y_i}$ can be written as

$$\forall i \in [\![1, n]\!],\ \mathbf{y_i} \underset{\text{i.i.d.}}{\sim} \mathcal{F}(\cdot, \boldsymbol{\theta_i}) + \boldsymbol{\xi_i} \ . \tag{4}$$

Without any other hypothesis, the outcomes of $\boldsymbol{\xi_i}$ (labeled $(\xi_{ij})_{j\in[\![1,N_i]\!]}$) are different for each individual and for each observation, with N_i the number of observations points of the i-th specimen. The global mixed-effects models for the j^{th} output measure of the i^{th} individual y_{ij} reads as

$$y_{ij} = \mathcal{F}(t_{ij}, \theta_i) + \xi_{ij} \ . \tag{5}$$

For the sake of simplicity, $f_{\boldsymbol{\Theta},\boldsymbol{\Pi}}$ is chosen to be a multivariate Gaussian distribution of dimension d:

$$f_{\boldsymbol{\Theta},\boldsymbol{\Pi}} \coloneqq \mathcal{N}(\boldsymbol{\mu}, \boldsymbol{\Sigma}) \ , \tag{6}$$

with $\boldsymbol{\mu} \in \mathbb{R}^d$ the mean vector and $\boldsymbol{\Sigma} \in \mathcal{M}_d(\mathbb{R})$ the covariance matrix. The individual parameters can be written

$$\boldsymbol{\theta_i} \coloneqq \boldsymbol{\mu} + \mathbf{b}_i \ , \tag{7}$$

with $\mathbf{b_i} \underset{\text{i.i.d.}}{\sim} \mathcal{N}(0, \mathbf{\Sigma})$. Here, $\boldsymbol{\mu}$ stands for the fixed effects (the same for the whole population) and $\mathbf{b}_i$ the random effects (different for each individual). The second hypothesis is that for each individual and each measure, the error term is a Gaussian white noise (no bias, no correlation):

$$\xi_{ij} \underset{\text{i.i.d.}}{\sim} \mathcal{N}(0, \omega_{ij}^2) \, , \tag{8}$$

with ω_{ij} the standard deviation of the noise of the j^{th} output measure of the i^{th} individual. Furthermore, the noise is supposed to be homoscedastic, *i.e.* $\omega_{ij} = \omega_i \; \forall \; j \in [\![1, N_i]\!]$.

Finally, the vector of parameters to be calibrated is denoted $\mathbf{\Psi}$:

$$\mathbf{\Psi} \coloneqq \Big(\boldsymbol{\mu}, \quad \mathbf{\Sigma}, \quad \mathbf{\Omega} \Big) \, ,$$

with $\mathbf{\Omega} = \text{diag}(\omega_1^2, \ldots, \omega_n^2)$. The mixed-effects models seek $\mathbf{\Psi}$ and provide an estimate of the individual parameters $(\boldsymbol{\theta_i})_{i \in [\![1,n]\!]}$ as a by-product.

2.2 Likelihood of the mixed-effects

The calibration is often achieved by maximizing the likelihood of $\mathbf{\Psi}$, $\mathcal{L}(\mathbf{\Psi}) \coloneqq f(\mathbf{y}_1, \ldots, \mathbf{y}_n | \mathbf{\Psi})$ (f is a generic letter for probability density functions or PDFs), even if other methods can be found to estimate $\mathbf{\Psi}$ [6] . The step-by-step derivation of the likelihood function can be found in [18]. Under the assumption of independent individuals, it reads as the product of all the individual likelihoods $\mathcal{L}_i(\mathbf{\Psi}) \coloneqq f(\mathbf{y}_i | \mathbf{\Psi})$,

$$\mathcal{L}(\mathbf{\Psi}) \coloneqq \prod_{i=1}^{n} \mathcal{L}_i(\mathbf{\Psi}) \, . \tag{9}$$

Because the $\boldsymbol{\theta_i}$'s are not observed, the likelihood of the i^{th} individual $\mathcal{L}_i(\mathbf{\Psi})$ is the integral of the marginal likelihood (*i.e.* the density of the output data $\mathbf{y}_i$ given individual parameters $\boldsymbol{\theta}_i$ and parameters $\mathbf{\Psi}$) $f(\mathbf{y}_i | \boldsymbol{\theta_i}, \mathbf{\Psi})$ with respect to all possible $\boldsymbol{\theta_i}$ over $\mathbb{R}^d$:

$$\mathcal{L}_i(\mathbf{\Psi}) \coloneqq \int_{\mathbb{R}^d} f(\mathbf{y}_i | \boldsymbol{\theta_i}, \mathbf{\Psi}) f(\boldsymbol{\theta_i} | \mathbf{\Psi}) \mathrm{d}\boldsymbol{\theta_i} \, . \tag{10}$$

In Eq. (10), $f(\boldsymbol{\theta_i} | \mathbf{\Psi})$ refers to the PDF of the model parameters distribution computed for the individual parameters.

The maximum likelihood estimator $\hat{\mathbf{\Psi}}$ is the result of the following maximization problem over the set of all the possible parameters Ξ:

$$\hat{\mathbf{\Psi}} \coloneqq \underset{\mathbf{\Psi} \in \Xi}{\arg\max} \, \mathcal{L}(\mathbf{\Psi}) \, . \tag{11}$$

In practice, the logarithm of the likelihood is computed to ease the numerical optimization [10].

2.3 Mixed-effects for multivariate models

The calibration of mixed-effects for univariate models has been extensively discussed [8, 20, 25]. This happens when only one measure is available on each specimen. Yet, sometimes, one has access to several measures on the same specimen (with longitudinal and transverse gauges or digital image correlation for instance). Then, the model to be calibrated becomes multivariate in the sense that the output is no longer a scalar but rather a vector, requiring to adapt the equation governing mixed-effects.

Let us note m_i the number of output measures of the i-th individual and $k \in [\![1, m_i]\!]$ the corresponding index. In the following, all specimens are supposed to have the same number of output measures, so $m_i = m \; \forall i \in [\![1, n]\!]$. All measures are supposed to have the same number of observation points N_i. The main difference with Section 2.1 is that the model output of each observation point is no longer a scalar y_{ij} but a vector $\mathbf{y}_{ij} \in \mathbb{R}^m$. The same occurs for the error term, now labeled $\boldsymbol{\xi}_{ij}$.

The equations governing the mixed-effects are [8, 20, 25]:

$$\begin{cases} \forall (i,j) \in [\![1,n]\!] \times [\![1,N_i]\!] \, , \mathbf{y}_{ij} = \mathcal{F}(t_{ij}, \boldsymbol{\theta}_i) + \boldsymbol{\xi}_{ij} \, , & \text{(12a)} \\ \forall i \in [\![1,n]\!], \boldsymbol{\theta_i} \underset{\text{i.i.d.}}{\sim} f_{\boldsymbol{\Theta},\boldsymbol{\Pi}} \, , & \text{(12b)} \\ \forall (i,j) \in [\![1,n]\!] \times [\![1,N_i]\!] \, , \boldsymbol{\xi}_{ij} \underset{\text{i.i.d.}}{\sim} \mathcal{N}(\mathbf{0}_{\mathbb{R}^m}, \boldsymbol{\Omega}_{ij}) \, , & \text{(12c)} \end{cases}$$

with $\mathbf{0}_{\mathbb{R}^m}$ the zero vector of $\mathbb{R}^m$ and $\boldsymbol{\Omega}_{ij}$ the covariance matrix of the error term which describes both the errors of the different sensors and the possible correlations between the errors on two different sensors. As in [21], the observations are supposed serially uncorrelated, meaning that the measurement errors at two different observation times are independent :

$$\forall i \in [\![1,n]\!], \; \forall (j_1, j_2) \in [\![1,N_i]\!]^2, \; j_1 \neq j_2 \Rightarrow Cov(\boldsymbol{\xi}_{ij_1}, \boldsymbol{\xi}_{ij_2}) = 0 \, . \tag{13}$$

Furthermore, for all specimens, the noise is supposed to be homoscedastic, that is to say : $\boldsymbol{\Omega}_{ij} = \boldsymbol{\Omega}_i \; \forall \; j \in [\![1, N_i]\!]$. Note that the only difference between Eqs. (5) and (12a) is that all terms are now vectors rather than scalars and that Eq. (12c) is the analogous of Eq. (8) for vectors instead of scalars.

Let us define for all individuals $\mathbf{Y}_i$, the matrix of the output data of the i-th specimen with $\mathbf{Y}_i \coloneqq (\mathbf{y}_{i1}, \ldots, \mathbf{y}_{iN_i}) \in \mathcal{M}_{m,N_i}(\mathbb{R})$. The rows of $\mathbf{Y}_i$ correspond to $\mathbf{y}_i^k = (y_{ij}^k)_{j \in [\![1,N_i]\!]}$, that is to say the N_i observations of the k-th measure of the i-th specimen. Similarly, it is possible to define the matrix of the errors as $\boldsymbol{\xi}_i \coloneqq (\boldsymbol{\xi}_{i1}, \ldots, \boldsymbol{\xi}_{iN_i}) \in \mathcal{M}_{m,N_i}(\mathbb{R})$. The rows of $\boldsymbol{\xi}_i$ matrix correspond to $\boldsymbol{\xi}_i^k = (\xi_{ij}^k)_{j \in [\![1,N_i]\!]}$ and can be understood as the N_i measurement errors of the k-th measure for the i-th specimen. Let us define $\widetilde{\mathbf{Y}}_i$ the flattened array by row of the matrix of the output data $\mathbf{Y}_i$ and the same for the matrix of the error term $\widetilde{\boldsymbol{\xi}}_i$. Then, $\widetilde{\mathbf{Y}}_i$ and $\widetilde{\boldsymbol{\xi}}_i$ belong to $\mathbb{R}^{mN_i}$. This allows to transform Eq. (12) into

$$\begin{cases} \forall i \in [\![1,n]\!], \widetilde{\mathbf{Y}}_i = \mathcal{F}(\mathbf{t}_i, \boldsymbol{\theta}_i) + \widetilde{\boldsymbol{\xi}}_i \, , & \text{(14a)} \\ \forall i \in [\![1,n]\!], \boldsymbol{\theta}_i \underset{\text{i.i.d.}}{\sim} f_{\boldsymbol{\Theta},\boldsymbol{\Pi}} \, , & \text{(14b)} \\ \forall i \in [\![1,n]\!], \; \widetilde{\boldsymbol{\xi}}_i \underset{\text{i.i.d.}}{\sim} \mathcal{N}(\mathbf{0}_{\mathbb{R}^{mN_i}}, \widetilde{\boldsymbol{\Omega}}_i) \, . & \text{(14c)} \end{cases}$$

with $\widetilde{\boldsymbol{\Omega}}_i = \boldsymbol{\Omega}_i \otimes I_{N_i}$ where $\otimes$ denotes the Kronecker product, I_{N_i} the identity matrix of $\mathcal{M}_{N_i}(\mathbb{R})$ and $\mathbf{0}_{\mathbb{R}^{mN_i}}$ the zero vector of $\mathbb{R}^{mN_i}$. Hence, the set of the model parameters to be calibrated, labeled $\boldsymbol{\Psi}$ is defined as :

$$\boldsymbol{\Psi} \coloneqq \Big(\boldsymbol{\mu}, \quad \boldsymbol{\sigma}, \quad \boldsymbol{\Omega}_1, \quad \ldots, \quad \boldsymbol{\Omega}_m \Big) \, .$$

Finally, the likelihood of the mixed-effects simply becomes $f(\widetilde{\mathbf{Y}}_1, \ldots, \widetilde{\mathbf{Y}}_n | \boldsymbol{\Psi})$. Eq. (10) remains the same except for $\mathbf{y}_i$ that becomes $\widetilde{\mathbf{Y}}_i$.

2.4 Likelihood estimation with Laplace approximation

The evaluation of the likelihood function requires to compute the individual likelihoods, which implies to estimate the multidimensional integral of Eq.(10). A fundamental method to compute the integral is the Monte-Carlo method [22]. However, such an approach requires too many model evaluations to keep the computational time reasonable. Thus, we rely on an alternative approach, the Laplace approximation [25].

The Laplace approximation [2, 25] applies to integrals of the type

$$A \coloneqq \int_{\mathbb{R}^d} \exp(-h(\mathbf{x}))\mathrm{d}\mathbf{x} \, ,$$

where $h(\cdot)$ is a function which must satisfy the following constraints:

1. $h(\cdot)$ admits a global minimum $\mathbf{x}_0$ that belongs to the integration interval,
2. $h(\cdot)$ is a twice-differentiable function,
3. its Hessian matrix $\mathcal{H}(h)$ computed at $\mathbf{x} = \mathbf{x_0}$ is a symmetric definite positive matrix.

The main idea is to assume that only points close to $\mathbf{x}_0$ significantly contribute to the integral, leading to the following Laplace approximation of A:

$$A \approx \exp(-h(\mathbf{x}_0)))\frac{(2\pi)^{\frac{d}{2}}}{\sqrt{|\mathcal{H}(h)(\mathbf{x}_0)|}} \, . \tag{15}$$

Given the modeling choices (Eq.(14)), the individual likelihoods read as :

$$\begin{aligned} \mathcal{L}_i(\boldsymbol{\Psi}) &= \int_{\mathbb{R}^d} f(\widetilde{\mathbf{Y}}_i|\boldsymbol{\theta_i}, \boldsymbol{\Psi}) f(\boldsymbol{\theta_i}|\boldsymbol{\Psi}) \mathrm{d}\boldsymbol{\theta_i} \\ &= \int_{\mathbb{R}^d} \frac{1}{\sqrt{|\widetilde{\boldsymbol{\Omega}}_i||\boldsymbol{\Sigma}|(2\pi)^{d+mN_i}}} \exp\left(-\frac{g_i(\boldsymbol{\mu}, \boldsymbol{\Delta}, \boldsymbol{\Lambda}_i, \widetilde{\mathbf{Y}}_i, \mathbf{b}_i)}{2}\right) \mathrm{d}\mathbf{b}_i \, . \end{aligned} \tag{16}$$

Here, $\boldsymbol{\Delta}$ is the transpose of the result of the Cholesky decomposition of $\boldsymbol{\Sigma}^{-1}$ (so $\boldsymbol{\Sigma}^{-1} = \boldsymbol{\Delta}^T\boldsymbol{\Delta}$), $\boldsymbol{\Lambda}_i$ is the transpose of the Cholesky decomposition of $\widetilde{\boldsymbol{\Omega}}_i^{-1}$ (so $\widetilde{\boldsymbol{\Omega}}_i^{-1} = \boldsymbol{\Lambda}_i^T\boldsymbol{\Lambda}_i$) and the function $g_i(\cdot)$ is defined by

$$g_i(\boldsymbol{\mu}, \boldsymbol{\Delta}, \boldsymbol{\Lambda}_i, \widetilde{\mathbf{Y}}_i, \mathbf{b}_i) \coloneqq \|\boldsymbol{\Lambda}_i(\widetilde{\mathbf{Y}}_i - \mathcal{F}(\mathbf{t}_i, \boldsymbol{\mu} + \mathbf{b}_i))\|^2 + \|\boldsymbol{\Delta}\mathbf{b}_i\|^2 \, . \tag{17}$$

The Laplace method is applied in two steps:

1. Search for the individual parameters (or rather the deviations), $\hat{\mathbf{b}}_i$, minimizing $g_i(\cdot)$ Eq. (17),
2. Computation of the Laplace approximation with Eq.(15).

To finalize the approximation of the likelihood, it remains to estimate the Hessian matrix of $g_i(\cdot)$ at $\hat{\mathbf{b}}_\mathbf{i}$ [25]:

$$\begin{aligned} \mathcal{H}(g_i)(\hat{\mathbf{b}}_i) = &\frac{\partial^2 \mathcal{F}(\boldsymbol{\mu}, \mathbf{t}_i, \hat{\mathbf{b}}_i)}{\partial \mathbf{b}_i \partial \mathbf{b}_i^T} \boldsymbol{\Lambda}_i^T \boldsymbol{\Lambda}_i (\widetilde{\mathbf{Y}}_i - \mathcal{F}(\boldsymbol{\mu}, \mathbf{t}_i, \hat{\mathbf{b}}_i)) \\ &+ \frac{\partial \mathcal{F}(\boldsymbol{\mu}, \mathbf{t}_i, \hat{\mathbf{b}}_i)}{\partial \mathbf{b}_i}^T \boldsymbol{\Lambda}_i^T \boldsymbol{\Lambda}_i \frac{\partial \mathcal{F}(\boldsymbol{\mu}, \mathbf{t}_i, \hat{\mathbf{b}}_i)}{\partial \mathbf{b}_i} + \boldsymbol{\Delta}^T\boldsymbol{\Delta} \, . \end{aligned} \tag{18}$$

In practice, $\frac{\partial^2 \mathcal{F}(\boldsymbol{\mu},\mathbf{t}_i,\hat{\mathbf{b}}_i)}{\partial \mathbf{b}_i \partial \mathbf{b}_i^T} \boldsymbol{\Lambda}_i^T \boldsymbol{\Lambda}_i (\widetilde{\mathbf{Y}}_i - \mathcal{F}(\boldsymbol{\mu}, \mathbf{t}_i, \hat{\mathbf{b}}_i))$ can be neglected if the model $\mathcal{F}(\cdot)$ is close enough to the experiment $\widetilde{\mathbf{Y}}_i$ [3]. The term $\frac{\partial \mathcal{F}(\boldsymbol{\mu},\mathbf{t}_i,\hat{\mathbf{b}}_i)}{\partial \mathbf{b}_i}$ is evaluated using a finite difference scheme. As a result, the negative log-likelihood is finally expressed as

$$\begin{aligned} -\ln(\mathcal{L}(\boldsymbol{\Psi})) &= -\sum_{i=1}^{n} \ln\left(\mathcal{L}_i(\boldsymbol{\Psi})\right) = -\sum_{i=1}^{n} \ln\left(\int_{\mathbb{R}^d} f(\widetilde{\mathbf{Y}}_i|\boldsymbol{\theta_i}, \boldsymbol{\Psi}) f(\boldsymbol{\theta_i}|\boldsymbol{\Psi}) \mathrm{d}\boldsymbol{\theta_i}\right) \\ &\approx \sum_{i=1}^{n} \left(\frac{1}{2} \ln(|\mathcal{H}(g_i)(\hat{\mathbf{b}}_i)|) + \frac{g_i(\boldsymbol{\mu}, \boldsymbol{\Delta}, \boldsymbol{\Lambda}_i, \widetilde{\mathbf{Y}}_i, \hat{\mathbf{b}}_i)}{2} + \frac{1}{2} \ln(|\widetilde{\boldsymbol{\Omega}}_i|(2\pi)^{mN_i}) \right) \\ &+ \frac{n}{2} \ln(|\boldsymbol{\Sigma}|) \ . \end{aligned} \tag{19}$$

2.5 Individual parameters estimation

The mixed-effects model also allows to infer the individual parameters. With the Laplace method, individual parameters are by-products of the likelihood function calculation given $\boldsymbol{\Psi}$. Once $\boldsymbol{\Psi}$ is chosen, the random effects $\mathbf{b}_i$ are estimated by looking for the dominating contribution in the individual likelihood $\mathcal{L}_i$ (Eq. (16)) through the minimization of function $g_i(\cdot)$ (Eq.(17))

$$\hat{\mathbf{b}}_i = \underset{\mathbf{b_i} \in \Xi}{\arg\min}\, g_i(\boldsymbol{\mu}, \boldsymbol{\Delta}, \boldsymbol{\Lambda}_i, \widetilde{\mathbf{Y}}_i, \mathbf{b}_i) \ , \tag{20}$$

with Ξ the research for the individual parameters. The individual deviations are then simply computed as $\boldsymbol{\theta_i} = \boldsymbol{\mu} + \mathbf{b}_i$.

2.6 Likelihood maximization estimate

Now that the expression of the likelihood for a mixed-effects model has been established, the model parameters can be identified by minimizing the opposite of the log-likelihood,

$$\hat{\boldsymbol{\Psi}} = \underset{\boldsymbol{\Psi} \in \Xi}{\arg\min} - \ln(\mathcal{L}(\boldsymbol{\Psi})) \ . \tag{21}$$

Remember that, as computing the likelihood is numerically challenging, the Laplace approximation of the likelihood is used instead in the optimization process. To solve the minimization problem (Eq. (21)), the first possibility would be to rely on gradient-based algorithms, which need either the gradient or an approximation of the gradient of the objective function. Here, the gradient of $-\ln(\mathcal{L}(\boldsymbol{\Psi}))$ expressed with Eq.(19) with respect to $\boldsymbol{\Psi}$ is difficult to compute analytically. Indeed the differentiation with respect to the population parameters of function $g_i(\cdot)$ requires to differentiate the individual deviations $\mathbf{b_i}$ defined in (20) with respect to the population parameters (*i.e.,* $\boldsymbol{\mu}$ and $\boldsymbol{\Sigma}$ *via* $\boldsymbol{\Delta}$).

A second possibility is to use gradient-free optimization algorithms, and in particular evolutionary algorithms. Though they require many likelihood estimations, they exhibit a greater ability to reach the global maximum of the likelihood, $\hat{\boldsymbol{\Psi}}$, despite the possible presence of local minima. The algorithm chosen here is the CMA-ES algorithm [12]. Given that a multivariate Gaussian distribution of dimension d (d stands for the number of parameters to be calibrated) is parametrized by at least d means and d variance parameters, and that mixed-effects models allow to estimate the variance of the error term, there is always at least $2d + 1$ to be estimated and thus $\ell \geqslant 2d + 1$.

The auxiliary optimization problem which identifies the individual parameters (the minimization of $g_i(\cdot)$

in Eq.(17)) is performed using the SLSQP algorithm [13].

3 Sequential calibration process

Advanced mechanical models characterize different aspects of the behavior of the material they describe, among which elasticity, viscosity, damage, *etc.* Each of these phenomena may be described by its own set of model parameters, which finally makes the number of parameters to be calibrated large (21 for the $3-d$ anisotropic elastic model for instance [4]). Consequently, a common practice [9, 23] in classical calibration consists into dividing the full calibration problem into calibration sub-problems that allow to identify different subsets of the complete parameters vector [14, 31]. In these works, the different sub-problems are associated with a specific part of the model parameters. The method consists into solving a sequence of calibration problems taking advantage in each step of the knowledge acquired so far. To be more precise, for a given step, in a frequentist framework, the coefficients calibrated in the previous steps are either taken as fixed inputs or severely bounded. In a Bayesian fashion, the identified posterior probability density on one step becomes a prior density for the next stages [28, 30].

The sequential approach requires to define a sequence of calibration sub-problems, which must be performed carefully. Indeed, as each step depends on the previous ones, an error on one step may flaw the whole calibration process. In some cases, the decomposition in sub-problems can be rather easy to perform with the help of expert knowledge [14, 31]. For example, [14] chooses to separate the model parameters between those that describe the electrical and mechanical behaviors of an energy harvester. Yet, in some cases, such a decomposition is not available. Consequently, not to depend on an arbitrary choice, another option consists into relying on a statistical criterion. For instance, given the available experiences, it can be decided to select the parameters to which the model output is sensitive following the analysis of the Fisher Information Matrix (the Hessian matrix of the log-likelihood) [16] resulting from the maximum likelihood estimation to define the sequence of interest.

In the mixed-effects framework, the objective is to characterize the material variability observed on a population of specimens modeled by the model parameters distribution. Following the decomposition of any PDF between marginals and copulas ([26]), the model parameters distribution $f_{\boldsymbol{\Theta},\boldsymbol{\Psi}}$ reads as :

$$f(\boldsymbol{\theta}_i|\boldsymbol{\Psi}) = c(F_1(\theta_i^1),\dots,F_d(\theta_i^d)|\boldsymbol{\Psi}_{cop}) \prod_{a=1}^{d} f_k(\theta_i^a|\boldsymbol{\Psi}_{marg}) \ , \tag{22}$$

with f_a the marginal of $\theta^a, a \in [\![1,d]\!]$, F_a the cumulative density function of $\theta_a, a \in [\![1,d]\!]$, $c(\cdot)$ the copula density function, $\boldsymbol{\Psi}_{marg}$ the parameters of the marginals (here mean and variance parameters) and $\boldsymbol{\Psi}_{cop}$ the parameters of the copula density (here the correlation coefficients) verifying $\boldsymbol{\Psi} = (\boldsymbol{\Psi}_{marg}, \boldsymbol{\Psi}_{cop})$. The decomposition of Eq.(22) allows to calibrate separately the different terms allowing a sequential calibration of $f_{\boldsymbol{\Theta},\boldsymbol{\Psi}}$. The sequential calibration process consists in defining a sequence of subsets of indices $\mathcal{S}_p \subset [\![1,d]\!]$ corresponding to the sensitive parameters defining the marginals and correlations parameters $\boldsymbol{\Psi}_p$ to be calibrated in step p, leading to the definition of a specific likelihood function $\mathcal{L}^p$. Once these parameters are estimated, a trust region $\mathcal{R}_p$ is defined. For the next stages, the parameters already estimated are limited to their trust region $\mathcal{R}_p$. This allows to ease the optimization as it focuses on a specific region of the parameter space, but also enables to make sure that the calibrated distribution remains consistent with the data used in the previous stages. The definition of the sequence

of calibration relies on the observation that the identification of a given marginal requires the model output to be enough sensitive to the corresponding parameter. This allows to design relevant experiments to estimate properly the PDF of interest. Figure 2 sums up the different stages of the method.

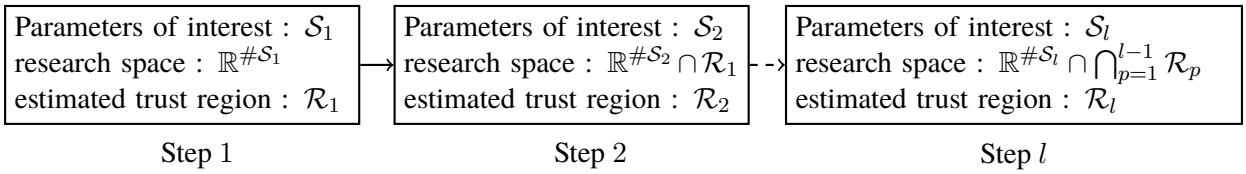

Figure 2: Different stages of the calibration process. A first calibration is performed to define trust region $\mathcal{S}_1$. In the second calibration problem, these parameters are identified again but limited to their trust region $\mathcal{R}_1$. The same procedure is repeated up to the complete identification of the model parameters distribution $f_{\boldsymbol{\Theta}}$. $\#E$ denotes the cardinality of set E.

4 Applications

This section presents the application of the considered sequential calibration to the identification of the orthotropic elastic model. After a brief description of the model in Section 4.1, the applied sequential strategy is exposed in Section 4.2 before describing the assessment protocol of the proposed method in Section 4.3 and presenting results in Section 4.5.

4.1 Orthotropic elastic model

This section aims to present the orthotropic elastic behavior of elementary unidirectional (UD) ply under the assumption of plane stress [4]. Let us note $\boldsymbol{\sigma} \coloneqq \begin{pmatrix} \sigma_{11}, & \sigma_{22}, & \sigma_{12} \end{pmatrix}$ the Cauchy stress (in MPa) and $\boldsymbol{\varepsilon} \coloneqq \begin{pmatrix} \varepsilon_{11}, & \varepsilon_{22}, & 2\varepsilon_{12} \end{pmatrix}$ the observed strain (without units). The orthotropic elastic model can be written in the material axis :

$$\begin{pmatrix} \varepsilon_{11} \\ \varepsilon_{22} \\ 2\varepsilon_{12} \end{pmatrix} = \underline{\underline{\mathbf{S}}} \begin{pmatrix} \sigma_{11} \\ \sigma_{22} \\ \sigma_{12} \end{pmatrix} = \begin{pmatrix} S_{11} & S_{21} & 0 \\ S_{12} & S_{22} & 0 \\ 0 & 0 & S_{66} \end{pmatrix} \begin{pmatrix} \sigma_{11} \\ \sigma_{22} \\ \sigma_{12} \end{pmatrix} , \tag{23}$$

with $\underline{\underline{\mathbf{S}}}$ the stiffness matrix. $\underline{\underline{\mathbf{S}}}$ is a symmetric matrix so $S_{12} = S_{21}$. For pratical interpretations, the coefficients of the stiffness matrix can be related to the elastic moduli, that is to say the longitudinal modulus E_{11}, the transverse modulus E_{22}, the shear modulus G_{12} and the Poisson's ratios ν_{12} and ν_{21} [4]. Finally, there are 4 parameters to be calibrated S_{11}, S_{22}, S_{12} and S_{66}.

4.2 Applying the sequential strategy

Given the modeling choices, the model parameters distribution is described by 14 parameters, namely 4 mean parameters, 4 variance parameters and 6 covariance parameters. Assuming that the elastic behavior in the fiber direction and in the matrix direction (described by S_{11} and S_{22}) are independent, we finally have 13 parameters to calibrate. The distribution parameters can be summed up into

$$\boldsymbol{\mu} = \begin{pmatrix} \mu_{S_{11}} \\ \mu_{S_{22}} \\ \mu_{S_{12}} \\ \mu_{S_{66}} \end{pmatrix} \quad \boldsymbol{\Sigma} = \begin{array}{c} \\ S_{11} \\ S_{22} \\ S_{12} \\ S_{66} \end{array} \begin{array}{c} \begin{array}{cccc} S_{11} & S_{22} & S_{12} & S_{66} \end{array} \\ \begin{pmatrix} \mathbb{V}(S_{11}) & * & * & * \\ 0 & \mathbb{V}(S_{22}) & * & * \\ Cov(S_{11}, S_{12}) & Cov(S_{22}, S_{12}) & \mathbb{V}(S_{12}) & * \\ Cov(S_{11}, S_{66}) & Cov(S_{22}, S_{66}) & Cov(S_{12}, S_{66}) & \mathbb{V}(S_{66}) \end{pmatrix} \end{array}, \tag{24}$$

where the $*$ indicate for the symmetric coefficient of the covariance matrix.

First, let us noticing that the orthotropic elastic model defined in Eq. (23) is characterized by 4 model parameters that may be identified from at most 3 strain profiles. Consequently, if the chosen load activates all model parameters (for instance $\boldsymbol{\sigma} = \sigma_0 \mathbf{1}_{\mathbb{R}^3}$, with $\mathbf{1}_{\mathbb{R}^3}$ the unitary vector of $\mathbb{R}^3$), the identification of the individual deviations $\mathbf{b}_i$ will be an ill-posed problem (Eq. (20)). This is of prime importance as it will impair the calibration results. Indeed, in the mixed-effects, the parameters of $f_{\boldsymbol{\Theta},\boldsymbol{\Pi}}$ are set to best fit the empirical distribution of the individual parameters. Nevertheless, the identifiability of the individual deviations $\mathbf{b}_i$ can be ensured when the model output is sensitive to only 3 of the 4 model parameters. Yet, only three of four coefficients can be identified at once, implying to set up a sequential strategy to get all non-zero coefficients detailed in Eq. (24)

Let us recall that to estimate a given marginal, it is necessary to have a proper estimation of the given parameter which requires the model output to be sensitive enough to the parameter in question. The same occurs for the estimation of the correlations that requires the model output to be sensitive enough to both the involved parameters.

For 0° UD laminate, let us consider the following load $\boldsymbol{\sigma} = \begin{pmatrix} \sigma_{11}, & 0, & \sigma_{12} \end{pmatrix}$. Such experiments correspond to multiaxial tests on tubular specimens combining both tension and torsion loads [5]. Then, following Eq. (23), the model output is determined by S_{11}, S_{12}, S_{66}. The application of previous remarks shows that it is possible to calibrate the parameters highlighted in red in Eq.(25):

$$\boldsymbol{\mu} = \begin{pmatrix} \mu_{S_{11}} \\ \mu_{S_{22}} \\ \mu_{S_{12}} \\ \mu_{S_{66}} \end{pmatrix} \quad \begin{array}{c} \\ S_{11} \\ S_{22} \\ S_{12} \\ S_{66} \end{array} \begin{array}{c} \begin{array}{cccc} S_{11} & S_{22} & S_{12} & S_{66} \end{array} \\ \begin{pmatrix} \mathbb{V}(S_{11}) & * & * & * \\ 0 & \mathbb{V}(S_{22}) & * & * \\ Cov(S_{11}, S_{12}) & Cov(S_{22}, S_{12}) & \mathbb{V}(S_{12}) & * \\ Cov(S_{11}, S_{66}) & Cov(S_{22}, S_{66}) & Cov(S_{12}, S_{66}) & \mathbb{V}(S_{66}) \end{pmatrix} \end{array}. \tag{25}$$

This allows to estimate a first trust region : $\mathcal{R}_1$. Let us now consider another load $\boldsymbol{\sigma} = \begin{pmatrix} 0, & \sigma_{22}, & \sigma_{12} \end{pmatrix}$. Such experiments correspond to multiaxial tests on tubular specimens combining both internal pressure and torsion loads [5]. Then, following Eq. (23), the model output is determined by S_{22}, S_{12}, S_{66}. The application of previous remarks shows that it is possible to calibrate the parameters highlighted in blue

in Eq.(25):

$$\boldsymbol{\mu} = \begin{pmatrix} \mu_{S_{11}} \\ \mu_{S_{22}} \\ \mu_{S_{12}} \\ \mu_{S_{66}} \end{pmatrix} \begin{matrix} S_{11} \\ S_{22} \\ S_{12} \\ S_{66} \end{matrix} \begin{pmatrix} S_{11} & S_{22} & S_{12} & S_{66} \\ \mathbb{V}(S_{11}) & * & * & * \\ 0 & \mathbb{V}(S_{22}) & * & * \\ Cov(S_{11},S_{12}) & Cov(S_{22},S_{12}) & \mathbb{V}(S_{12}) & * \\ Cov(S_{11},S_{66}) & Cov(S_{22},S_{66}) & Cov(S_{12},S_{66}) & \mathbb{V}(S_{66}) \end{pmatrix} . \tag{26}$$

Note that $\mu_{S_{12}}, \mu_{S_{66}}, \mathbb{V}(S_{12}), Cov(S_{12}, S_{66})$ and $\mathbb{V}(S_{66})$ are limited to trust region $\mathcal{R}_1$. This allows to estimate a second trust region ($\mathcal{R}_2$) for the calibrated parameters. All the distribution parameters of the model are now estimated through these two steps.

4.3 Testing the sequential strategy in the mixed-effects framework

To test the ability of the proposed methodology to calibrate the elastic model with mixed-effects, we choose to calibrate the model with synthetic data. Both the distribution parameters and the individual parameters are estimated.

A multivariate Gaussian distribution, defined by a mean vector $\boldsymbol{\mu}$ and a covariance matrix $\boldsymbol{\Sigma}$ is chosen to generate the synthetic data. This set of parameters will be denoted $\boldsymbol{\Psi}_{\text{exact}}$ in the following. Individual parameters $\boldsymbol{\theta_{i,\text{exact}}}$ are sampled from this distribution to compute, for each of these specimens the elastic model outputs $\boldsymbol{\varepsilon_{i,\text{exact}}}$. The mixed-effects approach is applied to the synthetic data and the results obtained are confronted to their exact counterpart.

The results are first compared at the population level to ensure that the model parameters distribution is properly estimated, using the relative error on the distribution parameters $\mathcal{E}(\hat{\boldsymbol{\Psi}})$, defined as

$$\mathcal{E}(\hat{\boldsymbol{\Psi}}) \coloneqq \Big(\mathcal{E}(\hat{\Psi}_1), \quad \ldots, \quad \mathcal{E}(\hat{\Psi}_\ell)\Big) \text{ with } \mathcal{E}(\hat{\Psi}_q) \coloneqq \frac{|\Psi_{\text{exact},q} - \hat{\Psi}_q|}{\Psi_{\text{exact},q}}, \forall q \in [\![1, \ell]\!] , \tag{27}$$

noting ℓ the number of distribution parameters, and the Kullback-Leibler divergence [17] $\text{KL}(f_{\boldsymbol{\Psi}_{\text{exact}}}, f_{\hat{\boldsymbol{\Psi}}})$ between the exact $f_{\boldsymbol{\Psi}_{\text{exact}}}$ and the calibrated distribution $f_{\hat{\boldsymbol{\Psi}}}$:

$$\text{KL}(f_{\boldsymbol{\Psi}_{\text{exact}}}, f_{\hat{\boldsymbol{\Psi}}}) \coloneqq \int_{\mathbb{R}^d} f_{\boldsymbol{\Psi}_{\text{exact}}}(\boldsymbol{\theta}) \ln\left(\frac{f_{\boldsymbol{\Psi}_{\text{exact}}}(\boldsymbol{\theta})}{f_{\hat{\boldsymbol{\Psi}}}(\boldsymbol{\theta})}\right) \mathrm{d}\boldsymbol{\theta} . \tag{28}$$

The adequation between the calibrated and the synthetic data can also be evaluated for each individual. To verify that the different specimens are correctly identified either in terms of calibrated individual parameters $\hat{\boldsymbol{\theta}}_{\boldsymbol{i}}$ or estimated output $\mathcal{F}(\mathbf{t}_i, \hat{\boldsymbol{\theta}}_{\boldsymbol{i}})$, the averaged relative error on the individual parameters $\mathbf{e}(\hat{\boldsymbol{\theta}}_{\mathbf{1}}, \ldots, \hat{\boldsymbol{\theta}}_{\boldsymbol{n}})$ is defined as:

$$\begin{aligned} &\mathbf{e}(\hat{\boldsymbol{\theta}}_{\mathbf{1}}, \ldots, \hat{\boldsymbol{\theta}}_{\boldsymbol{n}}) \coloneqq \frac{1}{n}\sum_{i=1}^{n} \mathbf{e}_i(\hat{\boldsymbol{\theta}}_{\boldsymbol{i}}) \text{ with } \mathbf{e}_i(\hat{\boldsymbol{\theta}}_{\boldsymbol{i}}) = \Big(e_i(\hat{\theta}_i^1), \quad \ldots, \quad e_i(\hat{\theta}_i^d)\Big) \\ &e_i(\hat{\theta}_i^a) = \frac{|\theta^a_{i,\text{exact}} - \hat{\theta}_i^a|}{\theta^a_{i,\text{exact}}} \ \forall a \in [\![1, d]\!], \end{aligned} \tag{29}$$

and the average error between the exact and estimated outputs $\mathbf{d}(\hat{\boldsymbol{\theta}}_{\mathbf{1}}, \ldots, \hat{\boldsymbol{\theta}}_{\boldsymbol{n}})$ for each strain component

$$\begin{aligned}&\mathbf{d}(\hat{\boldsymbol{\theta}}_{\mathbf{1}},\dots,\hat{\boldsymbol{\theta}}_{\boldsymbol{n}}) \coloneqq \Big(d_1(\hat{\boldsymbol{\theta}}_{\mathbf{1}},\dots,\hat{\boldsymbol{\theta}}_{\boldsymbol{n}}),\quad \dots,\quad d_m(\hat{\boldsymbol{\theta}}_{\mathbf{1}},\dots,\hat{\boldsymbol{\theta}}_{\boldsymbol{n}})\Big)\\ &\text{with } d_k(\hat{\boldsymbol{\theta}}_{\mathbf{1}},\dots,\hat{\boldsymbol{\theta}}_{\boldsymbol{n}}) \coloneqq \frac{1}{n}\sum_{i=1}^{n}\frac{1}{N_i}\|\boldsymbol{\varepsilon}^k_{\boldsymbol{i},exact} - \mathcal{F}^k(\mathbf{t}_i,\hat{\boldsymbol{\theta}}_{\boldsymbol{i}})\|_2 \;\forall k \in [\![1,m]\!]\,,\end{aligned} \tag{30}$$

are computed. Furthermore, to account for the specificity of the sampled specimens, the calibration is repeated 20 times with different individuals. The above indicators are averaged over the repetitions and their dispersion is characterized by the coefficient of variation COV(X) defined for any non-zero quantity X as $\text{COV}(X) = \frac{\sqrt{\widehat{V}(X)}}{\widehat{M}(X)}$ with $\widehat{M}(X)$ the empirical mean of X and $\widehat{V}(X)$ its empirical variance.

Finally, the maximum likelihood estimates (MLE) also enables to determine the variance of the error term. To keep the number of parameters reasonable and ease the minimization of the log-likelihood, it is decided here to assign to each specimen and measure the same covariance matrix of error term :

$$\forall i \in [\![1,n]\!]\ \boldsymbol{\Omega}_i = \boldsymbol{\Omega}\,.$$

4.4 Generating virtual data

The targeted means and standard deviations of the parameters are described in Table 1. Mean values are

Table 1: Exact values of the parameters distribution.

	S_{11} [MPa^{-1}]	S_{22} [MPa^{-1}]	S_{12} [MPa^{-1}]	S_{66} [MPa^{-1}]
Mean	8.52×10^{-6}	1.13×10^{-4}	-3.20×10^{-6}	2.37×10^{-4}
Standard deviation	6.09×10^{-7}	2.46×10^{-5}	5.27×10^{-7}	6.81×10^{-5}

consistent with material properties of T700M21 described in [19]. Standard deviations are chosen to allow material variability to express strongly. Yet, note that the dispersion of the material properties characterized by the selected standard deviations is greater than the variability observed on the experimental data. Several correlations scenarios are considered : independence (between S_{11} and S_{22}), positive correlation : $\rho(S_{11},S_{12}) = 0.54, \rho(S_{11},S_{66}) = 0.60, \rho(S_{12},S_{66}) = 0.91$ and negative correlations $\rho(S_{22},S_{12}) = -0.84, \rho(S_{22},S_{66}) = -0.70$ noting ρ the correlation.

For each of the 20 repetitions, 50 independent identically distributed vectors of parameters corresponding to 50 virtual specimens are sampled from $f_{\boldsymbol{\Psi}_{\text{exact}}}$ to achieve statistical consistency of the estimators. For each of these samples and given a stress profile (here a constant stress rate $\dot{\boldsymbol{\sigma}}_1 = \frac{\partial \boldsymbol{\sigma}_1}{\partial t}$ equal to $\Big(6.64,\quad 0,\quad 0.664\Big)$ MPa.s^{-1} and $\dot{\boldsymbol{\sigma}}_2 = \frac{\partial \boldsymbol{\sigma}_2}{\partial t}$ equal to $\Big(0,\quad 5.18,\quad 0.518\Big)$ MPa.s^{-1}), the corresponding model outputs $(\boldsymbol{\varepsilon}_{\boldsymbol{i},exact})_{i\in[\![1,n]\!]}$ are computed. An heteroscedastic noise is added to the experimental data:

$$\boldsymbol{\varepsilon}^j_{\boldsymbol{i},noisy} = \boldsymbol{\varepsilon}^j_{\boldsymbol{i},exact} \times (\mathbf{1}_{\mathbb{R}^3} + \beta\boldsymbol{\zeta}) \text{ with } \boldsymbol{\zeta} \sim \mathcal{N}(\mathbf{0}_{\mathbb{R}^3}, I_3) \text{ and } \beta = 0.02\,, \tag{31}$$

with $\mathbf{1}_{\mathbb{R}^3}$ the unitary vector of $\mathbb{R}^3$, $\mathbf{0}_{\mathbb{R}^3}$ the zero vector of $\mathbb{R}^3$ and I_3 the identity matrix of $\mathcal{M}_3(\mathbb{R})$. Yet, in the calibration process, the noise is considered as homoscedastic for all measures (*cf.* Eq.(8)). Exact and noisy data are depicted in Figure 3 for the first load profile.

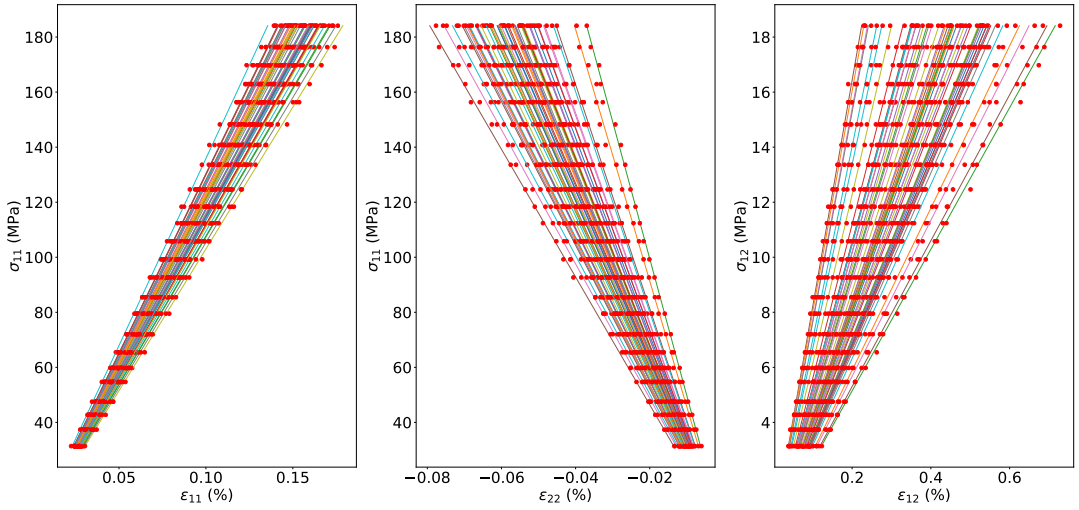

Figure 3: Example of a set of 50 synthetic stress-strain curves, without and with added noise (lines and dots, respectively).

4.5 Results

This section is dedicated to the presentation of the calibration results in the mixed-effects approach. First, the calibration results of step 1 are proposed to check that the joint distribution of S_{11}, S_{12} and S_{66} is properly estimated. Then, the results of the second stage are analyzed to assess the ability of the sequential procedure to estimate the full joint probability distribution.

4.5.1 Calibration of the joint distribution of S_{11}, S_{12} and S_{66}

Given the modeling assumptions described in Sections 4.2 and 4.4, there are $\ell = 12$ parameters to be calibrated : 3 mean parameters, 3 standard deviation parameters, 3 correlation parameters and 3 noise parameters. The calibration of the dependence structure is performed using the Cholesky decomposition of the covariance matrix [24], to make sure that the calibrated covariance matrix remains positive-definite. The optimization variables, $\mathbf{\Psi}$ are normalized between 0 and 1. 600 iterations of the CMA-ES algorithm are carried out to maximize the likelihood. The population of the CMA-ES algorithm is set to 12 following setting recommendations from [12]. For the determination of the individual parameters, 10 different initialization points are considered not to depend on the starting point.

The calibrated means, standard deviations and correlations are described in Table 4. These results indicate that all the distribution parameters are properly calibrated as the average relative error remains below 15% for all parameters in average over all repetitions. Furthermore, the coefficients of variation of the distribution parameters reach at most 20%, indicating that their range of variation is limited around the exact value. This is coherent with the low range of variation of the KL divergence displayed on Figure 4. These observations suggest that, regardless of the sampled specimens, for 50 individuals, the model parameters distribution is well estimated.

To check the consistency of the calibration, it is mandatory to study the calibration of the individual parameters as they influence the determination of the population parameters. Table 2 shows that all individual parameters are well estimated. This is confirmed by the magnitude of the error between the

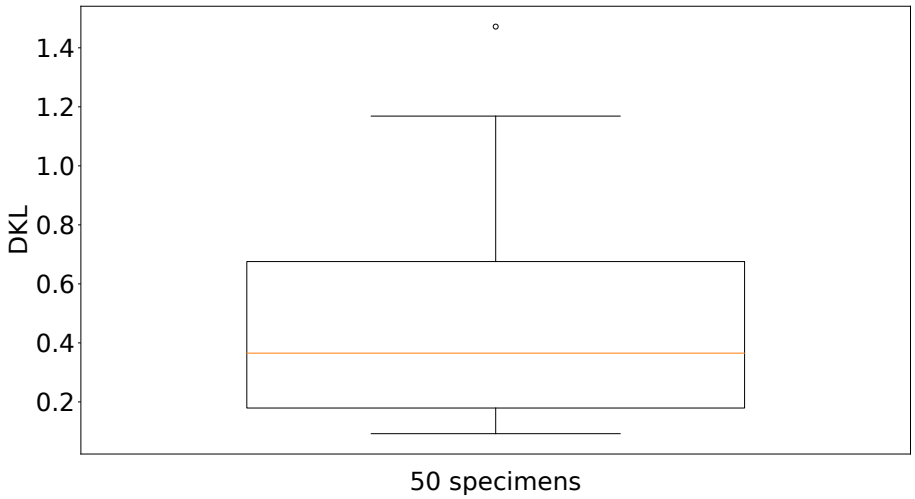

Figure 4: Boxplot of KL divergences of the calibrated distributions with respect to the exact distribution for the 20 repetitions.

exact data and model output for the calibrated parameters when compared to the range of values of the strain profile.

Thus, these different indicators allow to validate the calibration of joint distribution of S_{11}, S_{12} and S_{66} either at the population or specimen levels. Consequently, the first stage of the methodology is completed.

Table 2: Relative errors on the estimation of the individual parameters $\mathbf{e}(\hat{\boldsymbol{\theta}}_{\mathbf{1}}, \ldots, \hat{\boldsymbol{\theta}}_{\boldsymbol{n}})$ averaged over 20 repetitions of the calibration process. The corresponding coefficients of variation in % are indicated between brackets.

	S_{11} [MPa^{-1}]	S_{12} [MPa^{-1}]	S_{66} [MPa^{-1}]
Relative error (%)	$0.4(11)$	$0.4(10)$	$0.4(14)$

Table 3: Error in model space $\mathbf{d}(\hat{\boldsymbol{\theta}}_{\mathbf{1}}, \ldots, \hat{\boldsymbol{\theta}}_{\boldsymbol{n}})$ for each strain component.

Strain Component	ε_{11}	ε_{22}	ε_{12}
Order of magnitude of the mean strain value	10^{-4}	10^{-4}	10^{-3}
Distance in model space	3.54×10^{-10}	5.18×10^{-11}	1.10×10^{-8}

4.5.2 Calibration of the joint distribution of S_{22}, S_{12} and S_{66}

In the second stage of the methodology, the objective is to identify the joint distribution of S_{22}, S_{12} and S_{66}. Furthermore, the parameters of the joint distribution of S_{12} and S_{66} ($\mu_{S_{12}}, \mu_{S_{66}}, \mathbb{V}(S_{12}), \mathbb{V}(S_{66})$ and $Cov(S_{12}, S_{66})$), already estimated in the previous step will be limited to a trust region corresponding to $\mathcal{R}_1 = [0.8\boldsymbol{\Psi}_1, 1.2\boldsymbol{\Psi}_1]$. To implement bounds on $Cov(S_{12}, S_{66})$, a spherical decomposition of the covariance matrix is used [24]. The number of parameters remain the same (12), with 6 parameters

Table 4: Averaged calibrated mean, standard deviations and correlations $\mathbf{\Psi}_{1,\text{mean}}$ and averaged error $\mathcal{E}_{\text{mean}}(\hat{\mathbf{\Psi}}_1)$ over 20 repetitions of the calibration process with samples of 50 specimens each. The coefficients of variation COV in % are indicated between brackets.

	S_{11} [MPa^{-1}]	S_{12} [MPa^{-1}]	S_{66} [MPa^{-1}]
Exact Means	8.52×10^{-6}	-3.20×10^{-6}	2.37×10^{-4}
Averaged Calibrated Means	$8.52 \times 10^{-6}(2)$	$-3.24 \times 10^{-6}(4)$	$2.26 \times 10^{-4}(4)$
Averaged Errors On Calibrated Means (%)	$1(79)$	$3(78)$	$5(70)$
Exact Standard Deviations	6.09×10^{-7}	5.27×10^{-7}	6.81×10^{-5}
Averaged Calibrated Standard Deviations	$5.99 \times 10^{-7}(10)$	$5.21 \times 10^{-7}(10)$	$6.68 \times 10^{-5}(8)$
Averaged Errors On Calibrated Standard-Deviations (%)	$9(49)$	$8(75)$	$8(45)$
Correlations	$\rho(S_{11}, S_{12})$	$\rho(S_{11}, S_{66})$	$\rho(S_{12}, S_{66})$
Exact Correlations	0.54	0.60	0.91
Averaged Calibrated Correlations	$0.51(19)$	$0.58(15)$	$0.88(7)$
Averaged Errors On Calibrated Correlations (%)	$14(79)$	$11(85)$	$5(110)$

already limited to $\mathcal{R}_1$.

The calibrated means, standard deviations and correlations are described in Table 5. First, one can notice that the distribution parameters involving S_{22} (not calibrated in step 1) are well estimated. Indeed, the average relative error remains below 12% for all the coefficients in average over all the repetitions. Furthermore, the coefficients of variation of the distribution parameters reach at most 13%, indicating that their range of variation is limited around the exact value. Table 2 shows that all individual parameters are well estimated. This is confirmed by the magnitude of the error between the exact data and model output for the calibrated parameters when compared to the range of values of the strain profile.

It is important to notice that the estimation of the joint distribution of S_{12} and S_{66} (noted $f(S_{12}, S_{66})$ in the following) is not downgraded in the second stage. As a matter of fact, the average relative error of the corresponding parameters is comparable to its counterpart in the first step : the average relative error of $\mu_{S_{66}}$ reaches 5% in the first stage and 6% in the second stage for instance. The same occurs for all parameters defining $f(S_{12}, S_{66})$. This can also be assessed by comparing the KL divergence between the exact joint distribution of S_{12}, S_{66} ($f_{\text{exact}}(S_{12}, S_{66})$) and the calibrated distribution ($f_{\text{calibrated}}(S_{12}, S_{66})$) in the two stages as depicted Figure 5 for the 20 repetitions. It shows that the second estimation the joint distribution of S_{12} and S_{66} is not downgraded as the median of the KL divergences are comparable and that its estimation is slightly more accurate.

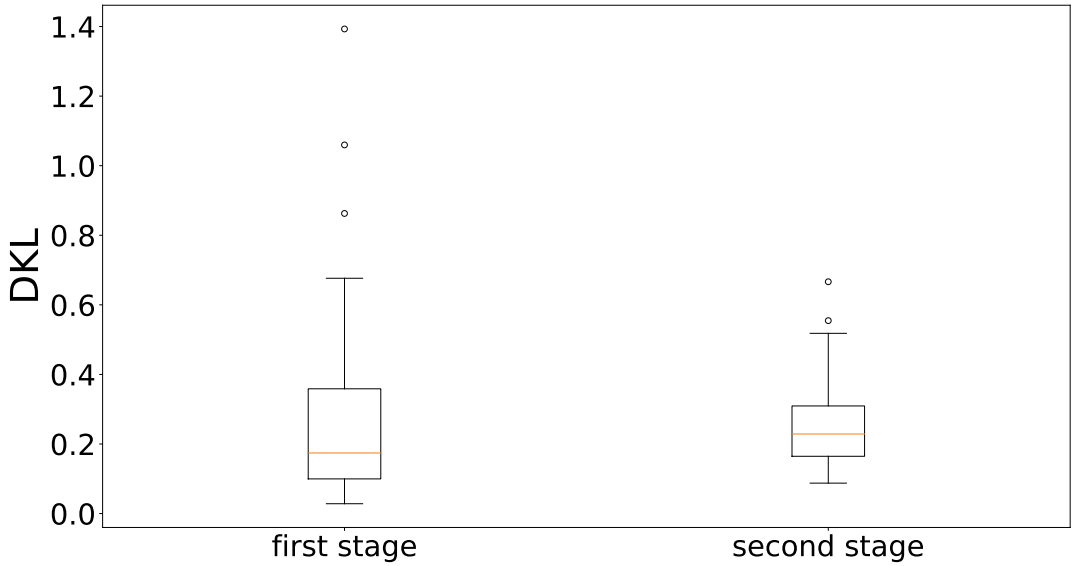

Figure 5: KL divergences of the calibrated and exact joint distribution S_{12} and S_{66} for the 20 repetitions in the two stages.

5 Conclusion

This article presents a sequential calibration procedure that aims to calibrate complex material models compliant with the mixed-effects framework using multivariate data. The method consists in defining a sequence of calibration sub-problems, each one corresponding to a subset of the available experimental data. The subdivision of the complete problem into sub-problems can be based on the choice of the expert and on sensitivity analyses. Indeed, well-chosen tests can activate different parts of the model, *i.e.* different subsets of the model parameters. Thus, each type of test makes it possible to define a sub-problem whose objective is to identify the joint distribution of a subset of the model parameters. A parameter can be involved in several sub-problems. In this case, it is identified once and the design domain of the corresponding distribution parameters is reduced to a trust region in the subsequent calibrations, to ensure consistency between the different sub-problems.

The method is applied to a virtual test case to the calibration of the orthotropic elastic model in plane stress. A first analysis of the material model shows the need to use such approaches because of the ill-posed nature of the full calibration problem. The joint distribution of the stiffness is sequentially estimated in two stages, using experiments performed on tubular specimens. The consistency of the results throughout the calibration process is ensured by bounding the parameters estimated twice. The results demonstrate the ability of the proposed procedure to estimate properly the model parameters distribution in the presence of significant material variability. Above all, this work shows that sequential calibration is compatible with mixed-effects models, allowing the calibration of complex non-linear models with mixed-effects for future works.

References

[1] Antoniadis Anestis and Carmona René. *Régression non linéaire et applications. (in french)*. Économie et statistiques avancées. Economica, Paris, 1992.

Table 5: Averaged calibrated mean, standard deviations and correltions $\mathbf{\Psi}_{2,\text{mean}}$ and averaged error $\mathcal{E}_{\text{mean}}(\hat{\mathbf{\Psi}}_2)$ over 20 repetitions of the calibration process with samples of 10 specimens each. The coefficients of variation COV in % are indicated between brackets.

	S_{22} [MPa^{-1}]	S_{12} [MPa^{-1}]	S_{66} [MPa^{-1}]
Exact Means	1.13×10^{-4}	-3.20×10^{-6}	2.37×10^{-4}
Averaged Calibrated Means	$1.08 \times 10^{-4}(6)$	$-3.14 \times 10^{-6}(3)$	$2.40 \times 10^{-4}(5)$
Averaged Errors On Calibrated Means (%)	3(71)	5(78)	6(74)
Exact Standard Deviations	2.40×10^{-5}	5.27×10^{-7}	6.81×10^{-5}
Averaged Calibrated Standard Deviations	$2.46 \times 10^{-5}(14)$	$5.34 \times 10^{-7}(11)$	$6.83 \times 10^{-5}(8)$
Averaged Errors On Calibrated Standard-Deviations (%)	11(79)	9(75)	6(95)
Correlations	$\rho(S_{22}, S_{12})$	$\rho(S_{22}, S_{66})$	$\rho(S_{12}, S_{66})$
Exact Correlations	-0.84	-0.70	0.91
Averaged Calibrated Correlations	$-0.84(6)$	$-0.68(14)$	0.91(3)
Averaged Errors On Calibrated Correlations (%)	12(69)	2(75)	5(72)

Table 6: Relative errors on the on the estimation of the individual parameters $\mathbf{e}(\hat{\boldsymbol{\theta}}_1, \ldots, \hat{\boldsymbol{\theta}}_n)$ averaged over 20 repetitions of the calibration process. The corresponding coefficients of variation in % are indicated between brackets.

	S_{22} [MPa^{-1}]	S_{12} [MPa^{-1}]	S_{66} [MPa^{-1}]
Relative error (%)	0.5(162)	0.3(1)	0.3(10)

[2] Adriano Azevedo-Filho and Ross Shachter. Laplace's method approximations for probabilistic inference in belief networks with continuous variables. pages 28–36, 1994.

[3] Douglas Bates, David Hamilton, and Donald Watts. Calculation of intrinsic and parameter-effects curvatures for nonlinear regression models. *Communications in Statistics - Simulation and Computation*, 12:469–477, 1983.

[4] J-M Berthelot. *Matériaux Composites—Comportement Mécanique et Analyse des Structures*. 01 2012.

[5] A.S. Chen and F.L. Matthews. A review of multiaxial/biaxial loading tests for composite materials. *Composites*, 24(5):395–406, 1993.

[6] M. Davidian and D.M. Giltinan. *Nonlinear Models for Repeated Measurement Data.* Chapman & Hall/CRC Monographs on Statistics & Applied Probability. Taylor & Francis, 1995.

Table 7: Error in model space $\mathbf{d}(\hat{\boldsymbol{\theta}}_1, \ldots, \hat{\boldsymbol{\theta}}_n)$ for each strain component.

	Independent Calibrations	Mixed-effects Without Covariance	Mixed-effects With Covariance
Strain Component	ε_{11}	ε_{22}	ε_{12}
Distance in model space	6.94×10^{-9}	1.98×10^{-08}	8.87×10^{-10}

[7] U.D.O. Defense, Technomic Publishing Company, Materials Sciences Corporation, American Society for Testing, and Materials. *Composite Materials Handbook-MIL 17, Volume III: Materials Usage, Design, and Analysis.* The Composite Materials Handbook-MIL 17. Taylor & Francis, 1999.

[8] Eugene Demidenko. *Mixed models. Theory and applications with R. 2nd ed.* 2013.

[9] A.S.o.M. Engineers. *Guide for verification and validation in computational solid mechanics*. ASME, 2006.

[10] R.A. Fisher and K. Pearson. *On an Absolute Criterion for Fitting Frequency Curves.* Messenger of mathematics. 1911.

[11] Mark Gallagher and John Doherty. Parameter estimation and uncertainty analysis for a watershed model. *Environmental Modelling & Software*, 22(7):1000–1020, 2007.

[12] Nikolaus Hansen, Sibylle Müller, and Petros Koumoutsakos. Reducing the time complexity of the derandomized evolution strategy with covariance matrix adaptation (CMA-ES). *Evolutionary computation*, 11:1–18, 2003.

[13] Steven G. Johnson. The nlopt nonlinear-optimization package.

[14] Byung C. Jung, Heonjun Yoon, Hyunseok Oh, Guesuk Lee, Minji Yoo, Byeng D. Youn, and Young Chul Huh. Hierarchical model calibration for designing piezoelectric energy harvester in the presence of variability in material properties and geometry. *Struct. Multidiscip. Optim.*, 53(1):161–173, jan 2016.

[15] Marc C. Kennedy and Anthony O'Hagan. Bayesian calibration of computer models. *Journal of the Royal Statistical Society: Series B (Statistical Methodology)*, 63(3):425–464, 2001.

[16] Taejin Kim and Byeng Dong Youn. Identifiability-based model decomposition for hierarchical calibration. *Structural and Multidisciplinary Optimization*, 60, 11 2019.

[17] S. Kullback and R. A. Leibler. On information and sufficiency. *The Annals of Mathematical Statistics*, 22(1):79 – 86, 1951.

[18] Clément Laboulfie, Mathieu Balesdent, Loïc Brevault, Sebastien Da Veiga, François-Xavier Irisarri, Rodolphe Le Riche, and Jean-François Maire. Calibration of material model using mixed-effects models. In *4th International Conference on Uncertainty Quantification in Computational Sciences and Engineering (UNCECOMP 2021)*, Athens, Greece, June 2021.

[19] Frédéric Laurin. Approche multiéchelle des mécanismes de ruine progressive des matériaux stratifiés et analyse de la tenue de structures composites (in french). 2005.

[20] Marc Lavielle. *Mixed Effects Models for the Population Approach: Models, Tasks, Methods and Tools.* 2014.

[21] John McFarland, Sankaran Mahadevan, Vicente Romero, and Laura Swiler. Calibration and uncertainty analysis for computer simulations with multivariate output. *AIAA Journal*, 46:1253–1265, 05 2008.

[22] Nicholas Metropolis and S. Ulam. The Monte Carlo method. *Journal of the American Statistical Association*, 44(247):335–341, 1949.

[23] William L. Oberkampf and Christopher J. Roy. *Verification and Validation in Scientific Computing*. Cambridge University Press, 2010.

[24] José Pinheiro and Douglas Bates. Unconstrained parametrizations for variance-covariance matrices. *Statistics and Computing*, 6:289–296, 09 1996.

[25] José Pinheiro and Douglas Bates. *Mixed-Effect Models in S and S-plus.*, volume 96. 2002.

[26] M. Sklar. *Fonctions de Répartition À N Dimensions Et Leurs Marges*. Université Paris 8, 1959.

[27] Albert Tarantola. *Inverse problem theory and methods for model parameter estimation.* Society for Industrial and Applied Mathematics, 1 edition, 2005.

[28] Angel Urbina, Thomas Paez, and Thomas Consulting. A bayes network approach to uncertainty quantification in hierarchically-developed computational models. *International Journal for Uncertainty Quantification*, 2, 01 2012.

[29] Larry Wasserman. *All of Statistics: A Concise Course in Statistical Inference.* Springer Publishing Company, Incorporated, 2010.

[30] Jiahui Ye, Mohamad Mahmoudi, Kubra Karayagiz, Luke Johnson, Raiyan Seede, Ibrahim Karaman, Raymundo Arroyave, and Alaa Elwany. Bayesian Calibration of Multiple Coupled Simulation Models for Metal Additive Manufacturing: A Bayesian Network Approach. *ASCE-ASME J Risk and Uncert in Engrg Sys Part B Mech Engrg*, 8(1), 10 2021. 011111.

[31] Byeng D. Youn, Byung C. Jung, Zhimin Xi, Sang Bum Kim, and W.R. Lee. A hierarchical framework for statistical model calibration in engineering product development. *Computer Methods in Applied Mechanics and Engineering*, 200(13):1421–1431, 2011.